Ferrite thin films: Synthesis, characterization and gas sensing properties towards LPG

ARTICLE *in* MATERIALS CHEMISTRY AND PHYSICS · JANUARY 2015

Impact Factor: 2.26 · DOI: 10.1016/j.matchemphys.2014.10.025

5 AUTHORS, INCLUDING:

D. M. Phase
UGC-DAE Consortium for Scientific Research
260 PUBLICATIONS **1,467** CITATIONS
SEE PROFILE

Rajeev Chikate
Abasaheb Garware College
50 PUBLICATIONS **1,219** CITATIONS
SEE PROFILE

Sunita Bhagwat
Abasaheb Garware College
7 PUBLICATIONS **24** CITATIONS
SEE PROFILE

Materials Chemistry and Physics 149-150 (2015) 333–338

Contents lists available at ScienceDirect

Materials Chemistry and Physics

journal homepage: www.elsevier.com/locate/matchemphys

Ferrite thin films: Synthesis, characterization and gas sensing properties towards LPG

Pratibha Rao [a], R.V. Godbole [a], D.M. Phase [b], R.C. Chikate [c], Sunita Bhagwat [a, *]

[a] Department of Physics, Abasaheb Garware College, Karve Road, Pune 411 004, India
[b] UGC-DAE CSR Centre, Indore, India
[c] Department of Chemistry, Abasaheb Garware College, Karve Road, Pune 411 004, India

HIGHLIGHTS

- (Co, Cu, Ni, Zn) ferrite thin films are synthesized by simple spray pyrolysis technique.
- Homogenization of substituent within ferrite structure.
- $CuFe_2O_4$ film exhibits predominantly ferrimagnetic nature.
- LPG sensing at lower temperature for $ZnFe_2O_4$ film.
- High sensitivity for $NiFe_2O_4$ film at higher temperature due to defects created in the structure.

ARTICLE INFO

Article history:
Received 10 June 2014
Received in revised form
27 September 2014
Accepted 15 October 2014
Available online 23 October 2014

Keywords:
Thin films
Crystal structure
Magnetic properties
Surface properties

ABSTRACT

Nanocrystalline (Co, Cu, Ni, Zn) ferrite thin films have been deposited onto the Si (100) and alumina substrates by spray pyrolysis deposition technique. Respective metal chlorides and iron chloride were used as precursors. The structural properties of (Co, Cu, Ni, Zn) ferrite thin films were investigated by X-ray diffraction (XRD) technique which confirms polycrystalline nature and single phase spinel structure. The surface morphology was studied using scanning electron microscopy (SEM) which reveals spherical morphology for these films except $NiFe_2O_4$ films that exhibit petal like structure. The optical transmittance and reflectance measurements were recorded using a double beam spectrophotometer. The optical studies reveal that the transition is direct band gap energy. The VSM analyzes reveal the predominant ferrimagnetic nature for $CuFe_2O_4$ films. The gas sensing properties towards Liquid Petroleum Gas (LPG) revealed that $ZnFe_2O_4$ films are sensitive at lower temperature while $NiFe_2O_4$ films show steep rise at higher temperature.

1. Introduction

Spinel ferrites have recently attracted considerable research interest on their structural, magnetic and electrical properties [1,2]. They are used in microwave devices, integrated circuits, reading/writing heads, sensors and catalytic material owing to their great magnetic permeability and dielectric constant, low dielectric loss at low frequencies, high Curie temperature as well as mechanical strength and chemical stability [3–5]. With the development of high-frequency and magnetic and magneto-optical memory devices of nano-structured materials having small dimensions, there has been a significant increase in the interest in ferrite thin films in recent years. There are many applications of ferrite thin films, such as gas or humidity sensors for which low density and nano-sized materials are required [6,7]. Properties of ferrite thin films are often found to be different from that of the bulk for various reasons such as crystallite size, high defect density, grain boundaries, texture, constraints caused by the substrate, and depend very much on fabrication parameters [8,9].

Cobalt ferrite ($CoFe_2O_4$) thin films have attracted much attention in recent years as one of the candidates for high density magnetic recording and magneto-optical recording media because of their unique physical properties such as high Curie temperature, large magnetic anisotropy, moderate magnetization and excellent chemical stability [10,11]. Copper ferrite ($CuFe_2O_4$) thin films also have excellent chemical stability, mechanical hardness, moderate saturation magnetization and high coercivity which can make it a good candidate for the electronic components used in computers,

* Corresponding author.
E-mail address: smb.agc@gmail.com (S. Bhagwat).

http://dx.doi.org/10.1016/j.matchemphys.2014.10.025
0254-0584/

recording devices, and magnetic cards [12]. Nickel ferrite ($NiFe_2O_4$) is a soft magnetic material with inverse spinel structure has great importance in high frequency power applications [13]. Zinc ferrite ($ZnFe_2O_4$) thin films have different applications such as photocatalyst material [14], gas sensors [15]. A recent investigation shows that the zinc ferrite, which is paramagnetic in the bulk form, becomes ferrimagnetic in nano-crystalline thin film form [16].

However, important problems that the researchers are concerned about are to fabricate ferrite films using a simple technology with low temperature heat treatment and low vacuum. To achieve potential applications, ferrite films have been fabricated earlier using various methods viz. RF sputtering [5], plasma laser deposition (PLD) [17] etc. These methods usually involve elaborate and costly apparatus and complicated process. Furthermore, the high deposition temperature limits the option of the substrate material as well as restricts different applications of ferrite thin films.

In view of this, we have employed spray pyrolysis technique to deposit ferrite thin films. This process is versatile and has the unique advantage of producing large surface-area films (about 2″ × 2″) at low cost. It involves a simple experimental setup and lowers the processing temperatures required to arrive at a stable phase. In the present work, (Co, Cu, Ni, Zn) ferrite thin films are deposited by spray pyrolysis technique on Si (100) and alumina and their structural, magnetic, optical and gas sensing properties were studied.

The films were deposited on Si (100) to study the magnetic properties of ferrite thin films. Si has attracted an attention as a substrate material due to its low cost and easy availability. An existence of about 35% mismatch in lattice constant between Si and ferrites and/or the formation of SiO_x buffer layer between Si and ferrite thin films during deposition leads to a high value of coercivity. This is also accompanied by the presence of lattice strain during the formation of ferrite thin films [18]. Alumina is well-known for its size and shape capability, high hardness, excellent wear and thermal shock resistance. High purity alumina is usable in both oxidizing and reducing atmospheres up to 1925 °C [19]. These properties make it the material of choice for sensing applications and therefore ferrite thin films were also deposited on alumina substrates.

2. Experimental

Nanocrystalline (Co, Cu, Ni, Zn) ferrite thin films were deposited using spray pyrolysis technique on Si (100) (5 mm × 2 mm) and alumina (5 mm × 5 mm) which were cleaned prior to the fabrication of ferrite thin films. Si wafers were dipped for 30 s in 1:20 HF:DI (De-ionized) water to remove the native oxide layer and any contamination in the oxide from the wafer surface and then strongly rinsed in DI water [20]. The alumina substrates were cleaned using soap solution, and then washed with distilled water, and later subjected to ultrasonicator bath and lastly dried under IR lamp [21]. An aqueous ethanol solution of a mixture of MCl_2 (M = Co, Cu, Ni, Zn) and $FeCl_3$ (mole ratio 1: 2) were chosen as the precursor solutions. Compressed air was employed as the carrier gas and the molar concentration of the precursor solution was kept 0.15 M. The solution was sprayed by a spray gun and the resulting mist was deposited on to the Si (100) and alumina by compressed air at a flow rate of 20 lpm. The substrates were kept at 350 °C during the deposition. The deposition time depends on the volume of the spraying solution. The nozzle-substrate distance was kept fixed at 30 cm. After deposition, the coated substrates were allowed to naturally cool down to room temperature before being taken out from the spray chamber. The deposited thin films were then air annealed at 650 °C for 3 h.

The structural characterization of the ferrite thin films deposited on Si (100) was carried out using Bruker AXS D8 diffractometer, with CuK_α radiation. Transmittance and reflectance measurements of all the films deposited on Si (100) were carried out using Perkin–Elmer spectrophotometer in 400–1100 nm range. Thicknesses of the ferrite films were measured using Talystep Profilometer and they were found to be about 2 μm for all the films. M–H curves of ferrite thin films deposited on Si (100) and annealed were recorded using LOT-Quantum Design MPMS SQUID VSM. The surface morphology of all the samples was studied using Jeol, JSM 6360A scanning electron microscope (SEM).

2.1. Gas sensitivity measurements

The gas-sensing characteristics of (Co, Cu, Ni, Zn) ferrite thin films deposited on alumina using spray pyrolysis and air annealed at 650 °C for 3 h was studied. The gas response was measured after providing the ohmic contacts using silver paste. Ferrite films were subjected for studying sensitivity of LPG towards the known amount using the static setup. The sensor material was kept in a steel chamber. The known amount (required ppm) of test gas was introduced in the chamber. The gas-sensing characteristics at different temperatures and concentrations were recorded using a Keithley 2400 source meter.

3. Results and discussion

3.1. Structural studies

The (Co, Cu, Ni, Zn) ferrite thin films were deposited at 350 °C on Si (100) and alumina substrates by spray pyrolysis and then air annealed at 650 °C for 3 h. The structural properties of these films were studied using X-ray diffraction (XRD) technique. Fig. 1 shows the XRD pattern of spray deposited and air annealed ferrite thin films on Si (100) at a glancing angle $\alpha = 0.3°$. The XRD patterns show single cubic spinel phase of the (Co, Cu, Ni, Zn) ferrite according to JCPDS card # 22-1086, 25-0283, 74-2081 and 82-1049 respectively. The average crystallite size, t, was determined using the Scherrer's formula [22] as given by equation (1) and are tabulated in Table 1.

$$t = \frac{0.9\lambda}{\beta \cos \theta_b} \quad (1)$$

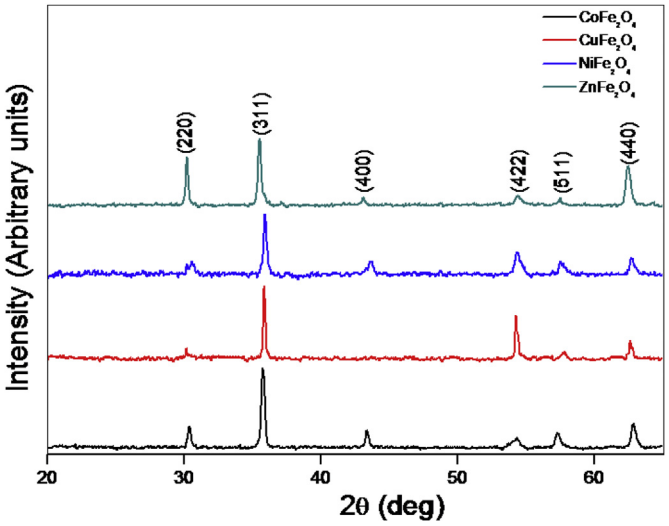

Fig. 1. XRD pattern of spray deposited and air annealed (Co, Cu, Ni, Zn) ferrite thin films.

Table 1
Structural and optical parameters of MFe_2O_4 (M = Co, Cu, Ni, Zn) ferrite thin films estimated from XRD and UV–VIS spectroscopy.

Sample	Crystallite size from XRD t (nm)	Lattice constant from XRD a (Å)	Lattice constant from JCPDS data a (Å)	Band gap from UV–VIS spectra E_g (eV)
$CoFe_2O_4$	54	8.338	8.391	1.86
$CuFe_2O_4$	67	8.327	8.349	1.71
$NiFe_2O_4$	46	8.305	8.337	1.80
$ZnFe_2O_4$	61	8.373	8.440	1.81

where β is the angular line width at half maximum intensity and θ_b is the Bragg angle for the actual peak.

The crystallite sizes of all ferrite thin films are found to be between 40 and 70 nm. The lattice constants of these films were calculated using indexing method [23] given by equation (2),

$$\frac{\lambda^2}{4a^2} = \frac{\sin^2\theta}{N} = \text{constant} \tag{2}$$

where $N = n^2(h^2 + k^2 + l^2)$. These lattice constants are also tabulated in Table 1. The lattice parameters of all the ferrite films do not match exactly with the standard JCPDS bulk values which could be attributed to the strains present on the surface of the films during the synthesis [24–26].

Quantitative information concerning the preferential crystal orientation is obtained from the texture coefficient (TC) [27] which can be calculated for different orientations using equation (3),

$$\mathrm{TC}(hkl) = \frac{I(hkl)/I_O(hkl)}{{}^1/_n \sum_n I(hkl)/I_O(hkl)} \tag{3}$$

where TC(hkl) is the texture coefficient of hkl plane, $I(hkl)$ is the measured intensity, $Io(hkl)$ is the relative intensity of the corresponding plane and n is the number of diffraction peaks considered.

TC of (220), (311), (422) and (440) planes of MFe_2O_4 (M = Co, Cu, Ni, Zn) ferrite thin films were calculated and tabulated in Table 2. From the values of TC(hkl), the domination of the crystallite orientation in the films could be described. It is observed that the preferential growth of all MFe_2O_4 (M = Co, Cu, Ni, Zn) ferrite thin films is in the (311) direction. (311) direction has the highest value of TC(hkl) than other directions for all the ferrite thin films. This could be attributed to the increase in structure factor which could be induced by the lattice deformation. It can also be confirmed from the deviation in lattice parameters (Pl. see Table 1).

3.2. Morphological studies

The spray deposited films had very good adherence to the substrates. Irregular morphology and agglomerates are observed in SEM images as shown in Fig. 2. SEM image of $CoFe_2O_4$ and $ZnFe_2O_4$ thin film deposited on Si (100) show spherical morphology. On the other hand, $NiFe_2O_4$ thin film exhibits petal like structure while $CuFe_2O_4$ possesses cubic morphology with spherical particles embedded in it.

Table 2
Texture coefficients of MFe_2O_4 (M = Co, Cu, Ni, Zn) ferrite thin films estimated from XRD.

Sample	TC (220)	TC (311)	TC (422)	TC (440)
$CoFe_2O_4$	0.6425	2.3424	0.2965	0.7191
$CuFe_2O_4$	0.3056	1.9681	1.1958	0.5309
$NiFe_2O_4$	0.5022	2.0729	0.8140	0.6106
$ZnFe_2O_4$	1.1807	1.6280	0.2315	0.9597

3.3. Optical studies

The optical properties of the 0.15 M spray deposited MFe_2O_4 (M = Co, Cu, Ni, Zn) thin films on Si (100) and air annealed at 650 °C for 3 h are shown in Fig. 3. These films show the transmission of about 70–80%.

The optical band gap is calculated using Tauc relation [28] given by equation (4),

$$\alpha h\nu = c(h\nu - E_g)^{1/2} \tag{4}$$

where 'c' is a constant, $h\nu$ is the photon energy and E_g is the band gap and the absorption coefficient α is given by equation (5)

$$\alpha = -\frac{1}{t}\ln\left[\frac{(1-R)^2}{T}\right] \tag{5}$$

where t is the thickness of the films.

A graph between $(\alpha h\nu)^2$ vs $h\nu$ is plotted and is shown in Fig. 4. The extrapolation of the linear portion of the plot of $(\alpha h\nu)^2$ vs $h\nu$ to the energy axis, gives the value of the energy band gap of film materials.

It can be seen that the plot varies linearly for all the films of ferrite in the region of strong absorption near the fundamental absorption edge. The linear variation of absorption coefficient of the ferrite thin films at high frequencies indicates that these thin films have direct transitions across the energy band gap. The values of energy band gap for MFe_2O_4 (M = Co, Cu, Ni, Zn) ferrite thin films lie between 1.7 and 1.9 eV and these are tabulated in Table 1. The values indicate that these films are semi-conducting oxides. $ZnFe_2O_4$, $CuFe_2O_4$ and $NiFe_2O_4$ thin films show higher values than the reported [29] whereas $CoFe_2O_4$ thin film shows similar value as reported earlier [30]. The increase in band gap in former ferrite thin films could be the effect of strain present in the films during deposition.

3.4. VSM studies

In this work, we have studied the magnetic properties of all the ferrite thin films deposited on Si (100) substrate and air annealed. Hysteresis curves for these films were recorded at 300 K between -8 kOe and +8 kOe and are shown in Fig. 5. The saturation magnetization (M_s), remanent magnetization (M_R) and coercivity (H_c) of all the ferrite thin films are tabulated in Table 3. The VSM analyses reveal the presence of a magnetic phase with very low saturation magnetization (M_s) and low coercivity (H_c) for all ferrite thin films. From Table 3, it can be seen that the saturation magnetization (M_s) is maximum for $CuFe_2O_4$ (10.47 emu/cc) and minimum for $ZnFe_2O_4$ (0.86 emu/cc).

This variation in M_s can be explained on the basis of the super exchange interaction mechanism. In a cubic system of ferrimagnetic spinels, the magnetic order is mainly due to super exchange interactions occurring between the metal ions in the A and B sublattices. Therefore, it is possible to vary magnetic properties of the thin films by varying the cations. This may be due to the fact that the exchange interaction between A and B sites gets lowered resulting in strengthening of B–B interaction and weakening of A–B interaction, which leads to decrease of saturation magnetization. Also this may be attributed to grain size, stress developed during the synthesis of the film and pinning effect as reported earlier [24–26]. The surface of the ferrite thin film could be

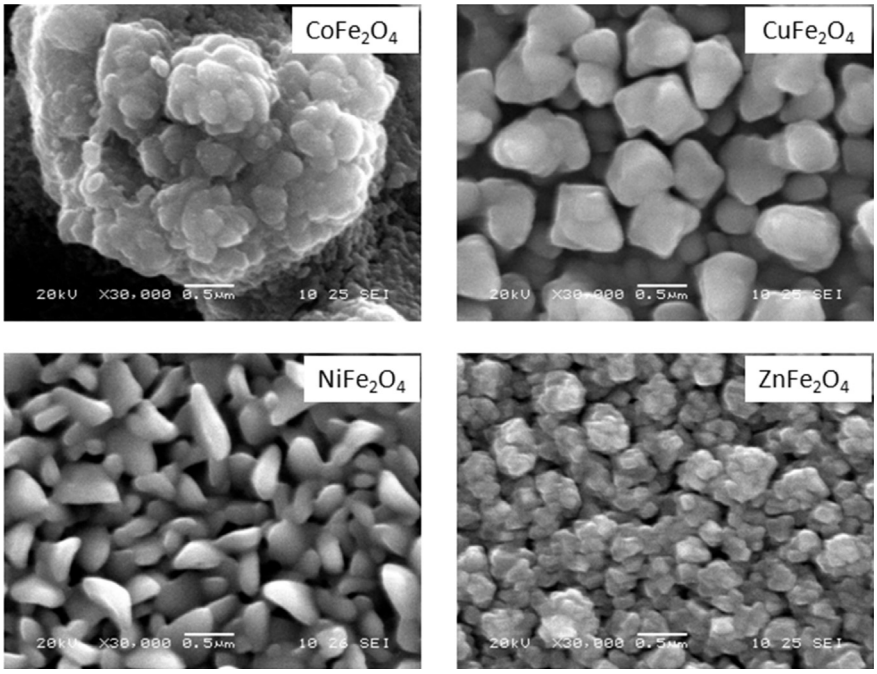

Fig. 2. SEM images of spray deposited and air annealed (Co, Cu, Ni, Zn) ferrite thin films.

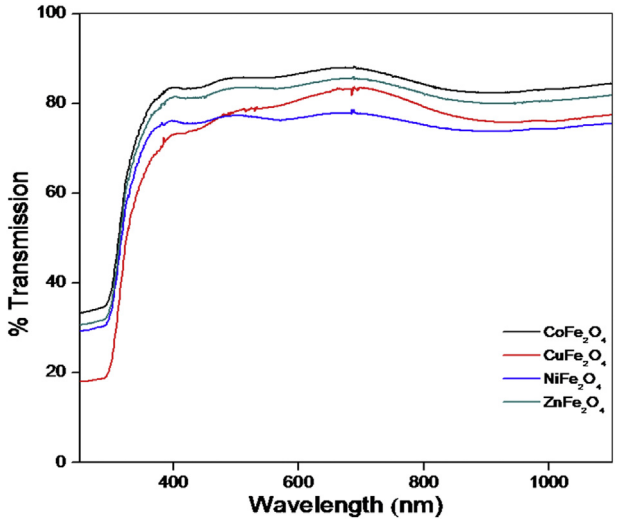

Fig. 3. Transmission spectra of spray deposited and air annealed (Co, Cu, Ni, Zn) ferrite thin films.

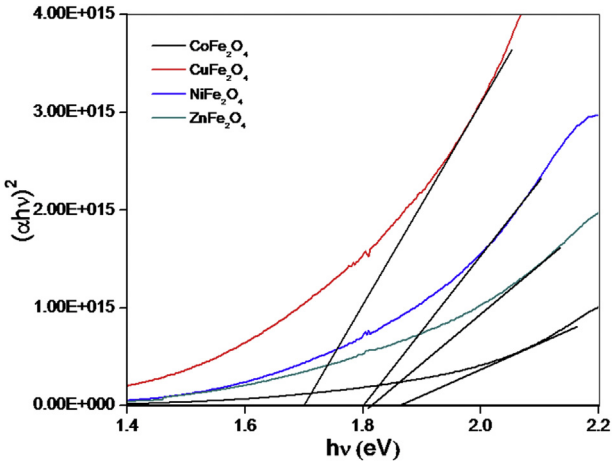

Fig. 4. Variation of $(\alpha h\nu)^2$ with photon energy $h\nu$ of spray deposited and air annealed (Co, Cu, Ni, Zn) ferrite thin films.

composed of some distorted or slanted spins that repel the core spins to align in the field direction; consequently, the overall domain structure is affected by the presence of stresses [10]. This affects the shape of hysteresis loop and its associated parameters.

The lowering in the magnetic behavior of $ZnFe_2O_4$ film could be due to the non-magnetic behavior of zinc. This can be explained on the basis of occupancy of more Zn atoms at B site than A site that eventually can be ascertained from lattice constants. It implies replacement of iron with zinc necessarily contributes for almost non-magnetic behavior for this material. The magnetic behavior of $CuFe_2O_4$ film can be explained on the basis of formation of two independent magnetic domains at A and B sites that exhibit ferri-magnetic nature through magnetic coupling interactions. It implies that Cu compete more for B site rather than A site that accounts for

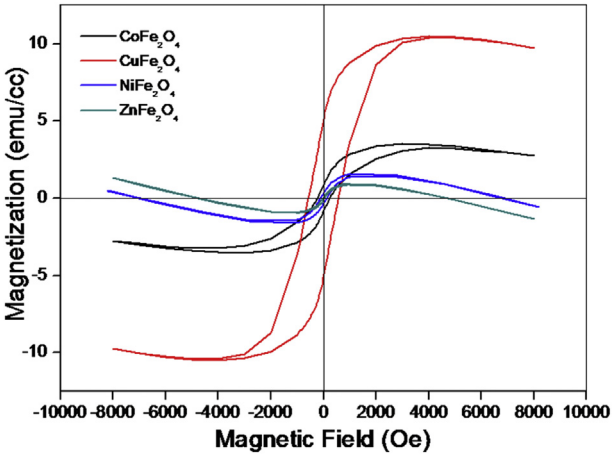

Fig. 5. VSM of spray deposited and air annealed (Co, Cu, Ni, Zn) ferrite thin films.

Table 3
Magnetic parameters of MFe_2O_4 (M = Co, Cu, Ni, Zn) ferrite thin films estimated from VSM.

Sample	Saturation magnetization M_s (emu/cc)	Remanent magnetization M_R (emu/cc)	Coercivity H_c (Oe)
$CoFe_2O_4$	3.12	0.92	224.5
$CuFe_2O_4$	10.47	5.38	575.2
$NiFe_2O_4$	1.46	0.35	113.4
$ZnFe_2O_4$	0.86	0.09	30.5

well defined hysteresis curve. For $CoFe_2O_4$ and $NiFe_2O_4$ films, it is plausible that the magnetic domains generated at A and B sites presumably interact through individual metal ions in antiferromagnetic fashion while collectively these two domains contribute towards effective magnetization.

Fig. 6 shows M–T curves of these films which were recorded up to 300 K (limiting value of the instrument) at constant magnetic field i.e. the saturation magnetization value. It shows that magnetization reduces continuously which can be attributed to magnetic relaxation [29]. When the system cooled down to 50 K under an applied field, the random magnetic moment vectors became parallel to magnetic field. When the temperature is increased magnetization decreases continuously due to misalignment of magnetic moment vectors.

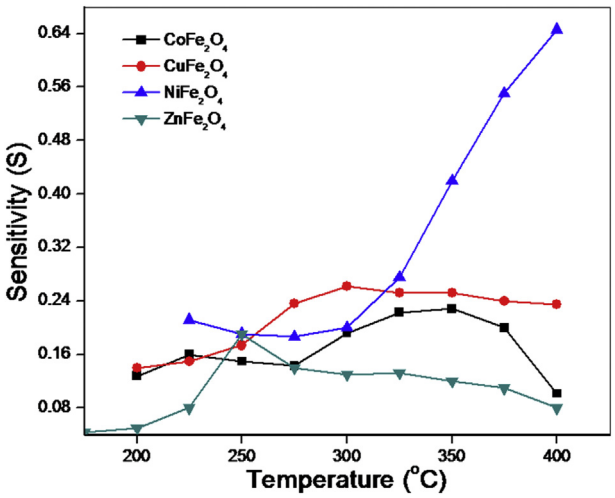

Fig. 7. Sensitivity of spray deposited and air annealed (Co, Cu, Ni, Zn) ferrite thin films for LPG at 5 ppm.

3.5. Gas sensing characteristics

The gas-sensing mechanism being the surface-controlled phenomena, the grain size, surface states, oxygen adsorption and the

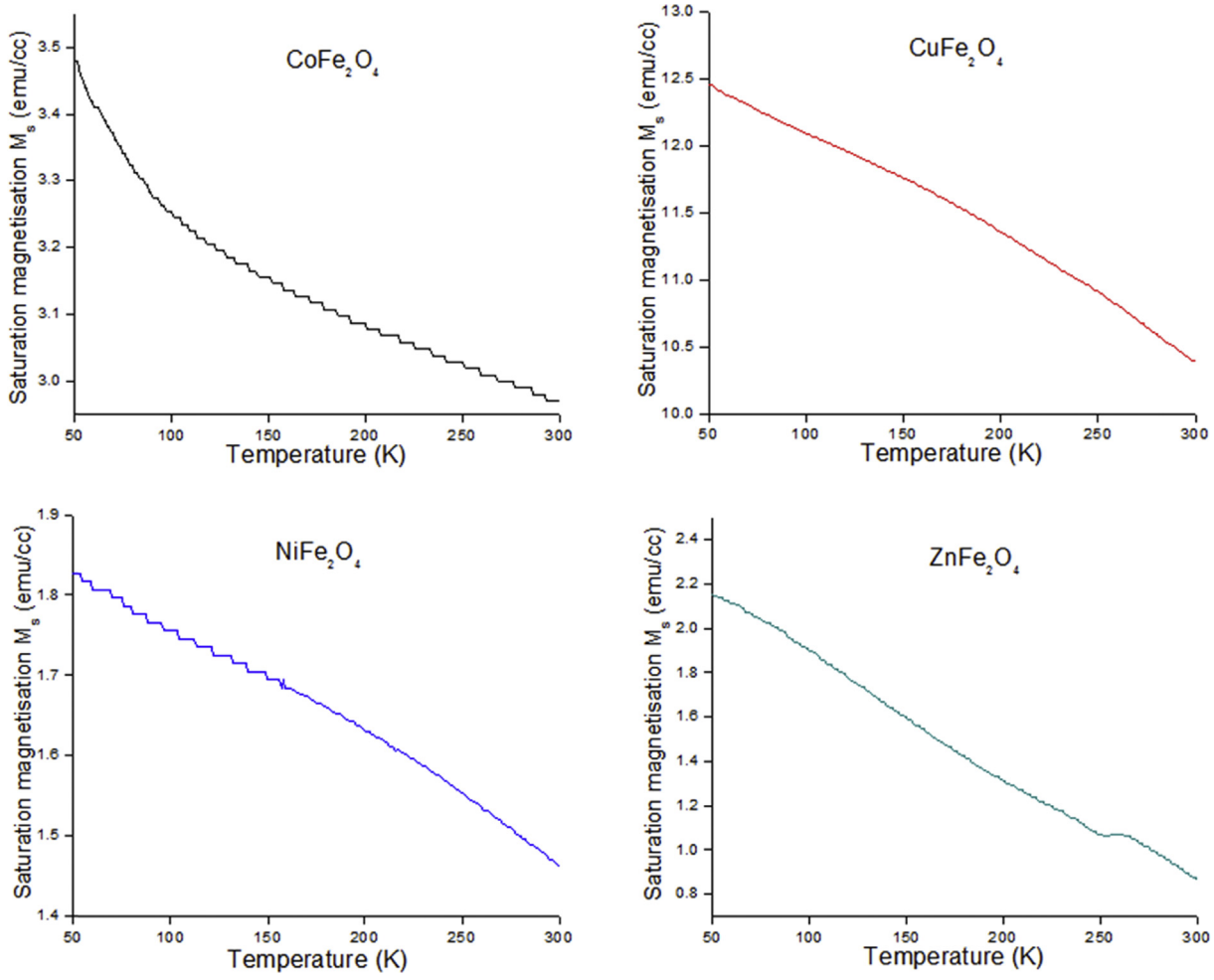

Fig. 6. M–T curves of spray deposited and air annealed (Co, Cu, Ni, Zn) ferrite thin films.

lattice defects play an important role. Thin film has advantage like high surface area, fast recovery, lower energy input, device compatibility, miniaturization and overall cost effectiveness. The gas sensitivity is greatly influenced by temperature. Ferrites mostly sense gases at higher temperatures. The oxygen species in the form of O^- and O^{2-} on the ferrite surface play an important role in the gas-sensing phenomena. The studies on ferrite thin films as potential gas sensors have carried out for the possibility of using these ferrite films for the detection of LPG. The sensitivity of the ferrite thin films are calculated when they are exposed to 5 ppm of LPG.

All the ferrite films are p-type semiconducting oxides as all films respond to LPG by increase in the electrical resistance [31]. The combustion of LPG; which is a hydrocarbon containing CH_4, C_3H_8 and C_4H_{10} with reducing hydrogen species bound to carbon atoms, might be taking place. It may result in the formation of CO, CO_2 and H_2O with the release of electrons for the conduction which causes electrons to enter into the conduction band of oxide and recombine with the holes giving rise to decrease in the conductivity. The gas response, sensitivity (S) [31,32] for a given test gas is calculated using equation (6):

$$S = \frac{R_a - R_g}{R_a} \tag{6}$$

where R_a and R_g are the electrical resistances of the sensor in air and in test gas respectively.

Fig. 7 shows the sensitivity variation towards LPG of all ferrite films as a function of the temperature. All the sensors do not seem to have any appreciable sensitivity up to about 150 °C. Above 150 °C the $ZnFe_2O_4$ sensor element starts responding to the gas as shown. It is seen that the element senses LPG with a lower sensitivity ~0.2 compared to all the other sensors and is attained at 250 °C.

$CuFe_2O_4$ sensor starts responding to LPG only above 200 °C and reaches a maximum in the sensitivity ~0.26 at 300 °C. In the case of the sensing characteristics of $NiFe_2O_4$, we do observe sensitivity but could not get exact operating temperature till 400 °C. It is observed that the sensor starts responding drastically to LPG only above 300 °C and this sensitivity keeps on increasing even above 400 °C. $CoFe_2O_4$ show sensitivity ~0.22 for LPG at higher temperature 350 °C as compared to other sensors.

Better sensitivity for LPG is observed for $ZnFe_2O_4$ at lower temperature; an essential feature for a thin film employed for its gas sensing properties. Although the crystallite size is found to be higher, its enhanced sensitivity is due to proper dispersion of Zn atoms within ferrite structure which is further corroborated with retention in the sensitivity up to 400 °C. However, $NiFe_2O_4$ exhibits good response at higher temperature probably due to creation of structural defects, small crystallite size and petal like morphology. It is feasible that during sensing experiments at higher temperatures, the catalytic surface of film is more exposed to Ni site rather than Fe site. This leads to substantial increase in sensing properties at higher temperature.

The plausible mechanism of LPG sensing by these films can be summarized as: (i) desorption of surface oxygen species (ii) oxidation of LPG induced by desorbed oxygenated species (iii) intermolecular electron transfer from LPG to film and (iv) recombination of hole and electron in the sensor material. These processes are simultaneously occurring on the surface of thin film in a synergistic manner.

4. Conclusions

Nanocrystalline (Co, Cu, Ni, and Zn) ferrite thin films have been successfully deposited onto Si (100) and alumina using low cost spray pyrolysis deposition technique. These films are post-annealed to obtain single phase spinel structure. SEM images of these films show spherical morphology for all ferrite films except nickel ferrite which shows petal like structure. The optical band gap of these thin films was found to be between 1.7 and 1.9 eV. The VSM analyze reveals the ferrimagnetic nature of the films. The combined effect of grain size, stress and type of cations is observed in MFe_2O_4 thin films from the VSM study. LPG sensing properties of these films suggest that $ZnFe_2O_4$ film is better suited as sensor at lower temperature and lower concentration due to homogenization of Zn atoms within ferrite lattice. However, $NiFe_2O_4$ film exhibits excellent sensing of LPG at high temperature as a consequence of formation of petal like morphology and generation of defects in the structure.

Acknowledgments

Authors would like to thank Department of Science and Technology (DST), India SR/S2/CMP-0035/2012 and University Grants Commission (UGC), India 42-778/2013 (SR) for the financial assistance. Authors are also grateful to UGC-DAE CSR, Indore for providing VSM facility.

References

[1] E.P. Naiden, V.A. Zhuravlve, V.I. Itin, O.G. Terekhova, A.A. Magaeva, YuF. Ivanov, Russ. Phys. J. 49 (2006) 946–951.
[2] Y.H. Hou, Y.J. Zhao, Z.W. Liu, X.C. Zhong, W.O. Qui, D.C. Zengl, L.S. Wen, J. Phys. D Appl. Phys. 43 (2010) 445003 (7pp).
[3] M. Seider, V. Matajee, T. Grygar, J. Khadlecova, Ceram. Int. 26 (2000) 507–512.
[4] A.M. Abdeen, J. Magn. Mater. 185 (1998) 199–206.
[5] M.A. Ahmed, N. Okasha, L. Salah, J. Magn. Magn. Mater. 164 (2003) 241–250.
[6] Y. Shimizu, M. Egashira, MRS Bull. 24 (1999) 18–24.
[7] C. Xu, T. Jun, N. Miura, N. Yamazoe, Chem. Lett. 3 (1990) 441–444.
[8] M. Ahmad, M. Desai, R. Khatirkar, J. Appl. Phys. 103 (2008) 013903 (4pp).
[9] X. Sui, M.H. Kryder, Appl. Phys. Lett. 63 (1993) 1582–1584.
[10] W.F.J. Fontijn, P.J. Vander Zaag, L.F. Feiner, R. Metselaar, M.A.C. Devillers, J. Appl. Phys. 85 (1999) 5100–5105.
[11] Y. Suzuki, Ann. Rev. Mater. Res. 31 (2001) 265–289.
[12] S.D. Sartale, C.D. Lokhande, M. Muller, Mater. Chem. Phys. 80 (2003) 120–128.
[13] A. Verma, D.C. Dube, J. Am. Ceram. Soc. 88 (2005) 519–523.
[14] A.A. Tahir, K.G.U. Wijayantha, J. Photochem, Photobiol. A: Chem. 216 (2010) 119–125.
[15] Z. Jiao, M. Wu, J. Gu, Z. Qin, IEEE Sensors J. 3 (2003) 435–438.
[16] Monica Sorescu, L. Diamandescu, R. Swaminathan, M.E. McHenry, M. Feder, J. Appl. Phys. 97 (2005) 10G105 (3pp).
[17] Gagan Dixit, J.P. Singh, R.C. Srivastava, H.M. Agrawal, R.J. Chaudhary, Adv. Mat. Lett. 3 (2012) 21–28.
[18] L. Iyengar, R.R. Prasad, B. Qadri, Curr. Sci. 42 (1973) 534–537.
[19] E. Dorre, H. Hubner, Alumina Processing, Properties and Applications Series: Materials Research and Engineering, Springer, Berlin Heidelberg, 2011.
[20] G.S. Higashi, Y.J. Chabal, G.W. Trucks, K. Raghavachari, Appl. Phys. Lett. 56 (1990) 656–658.
[21] A. Wisitsoraat, A. Tuantranont, E. Comini, G. Sberveglieri, W. Wlodarski, Thin Solid Films 517 (2009) 2775–2780.
[22] H.P. Klug, L.E. Alexander, X-ray Diffraction Procedures for Polycrystalline and Amorphous Materials, John Wiley, 1974.
[23] E.C. Subbarao, L.K. Singhal, D. Chakravorty, M.F. Merriam, V. Raghavan, Experiments in Materials Science, Tata Magraw Hill Publishing Co. Ltd., 1972.
[24] G. Dixit, J.P. Singh, R.C. Srivastava, H.M. Agarwal, R.S. Choudhary, A. Gupta, Ind. J. Pure Appl. Phys. 48 (2010) 287–291.
[25] J. Ding, Y.J. Chen, Y. Shi, S. Wang, Appl. Phys. Lett. 77 (2000) 3621–3623.
[26] A. Lisfi, C.M. Williams, J. Appl. Phys. 93 (2003) 8143–8145.
[27] S.A. Nasser, H.H. Afify, S.A. E-Hakim, M.K. Zayed, Thin Solid Films 315 (1998) 327.
[28] J. Tauc (Ed.), Amorphous and Liquid Semiconductors, Plenum, 1974.
[29] S.M. Chavan, M.K. Babrekar, S.S. More, K.M. Jadhav, J. Alloy Comp. 507 (2010) 21–25.
[30] C. Himcinschi, I. Vrejoiu, G. Salvan, M. Fronk, A. Talkenberger, D.R.T. Zahn, D. Rafaja, J. Kortus, J. Appl. Phys. 113 (2013) 084101 (8pp).
[31] C.V. Gopal Reddy, S.V. Manorama, V.J. Rao, J. Mater. Sci. Lett. 19 (2000) 775–778.
[32] N. Iftimie, E. Rezlescu, P.D. Popa, N. Rezlescu, J. Optoelec. Adv. Mater. 7 (2005) 911–914.